ACS OMEGA

Open Access

http://pubs.acs.org/journal/acsodf

Article

Interfacial Reinforcement of Polymer-Bonded Explosives by Grafting a Neutral Bonding Agent with Enhanced Mechanical Properties

Chengcheng Zeng,* Gang Li, Congmei Lin, Guansong He, Lixiao Hao, Feiyan Gong, Shengjun Zheng, and Fude Nie*

Cite This: *ACS Omega* 2025, 10, 9441−9452

Read Online

ACCESS | Metrics & More | Article Recommendations

ABSTRACT: The poor bonding of energetic crystals has severely influenced the comprehensive performance of explosive composites. Herein, surface modification is displayed as an effective method to implement the interaction of composites. In this work, a multipurpose functionalization of interfacial additives and biomimetic coating was demonstrated in facial and reproductive ways. The self-polymerization of dopamine (DA) formed polydopamine (PDA) shells, followed by neutral bonding agent (NBA) grafting, which led to a roughness change of the 1,3,5-triamino-2,4,6-trinitrobenzene (TATB) crystal. The new bonds of amino ester (−NHCOO) were generated, proving the success of the "grafting to" strategy. The ability to resist deformation after surface modification was significantly improved with strain below 0.06% under 75 °C or 9 MPa. The storage modulus of PBX is above 4000 MPa within a temperature range of 20−120 °C. Moreover, the mechanical properties of PBX-3 significantly improved, with the strength and elongation in the Brazillian mechanical test increasing by 19.4 and 24.4%, respectively, ultimately resulting in an enhancement of approximately 51.6% in fracture work. The dual effect of hydrogen bonding and a physical anchor may serve to enhance mechanical properties. The approach of PDA coating and NBA grafting presented in this paper may be favorable for improving the mechanics of general composites.

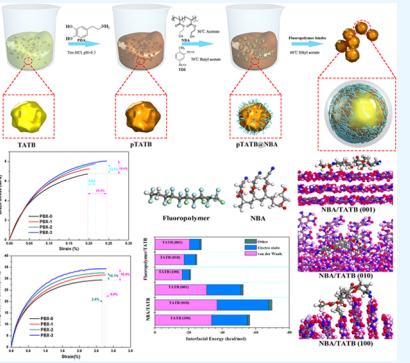

1. INTRODUCTION

Polymer-bonded explosives (PBXs) can be regarded as a composite with high-solid filling composed of explosive crystal and polymer binders, and the interface plays an overwhelming role in these multiphase materials.[1,2] Due to the significant difference between explosive particles and binders, the weak bonding work can seriously affect the mechanical and safe properties.[3,4] After macroscopic damage accumulates, the sensitivity and the detonation performance of explosives are influenced and further severely limit the application in civil and military fields.[5−8]

Neutral bonding agents (NBA) are commonly used as a "molecular bridge" in high-energy solid propellants. Due to the functional groups of −CN, −COO, and −OH on the molecular chain playing as interaction points, it has a strong affinity for other components and improves the interfacial interaction between solid fillers and binders.[9−11] Qin et al.[12] used molecular dynamics (MD) calculations to study the interaction work between NBA and 2,4,6,8,10,12-hexanitro-2,4,6,8,10,12-hexaazaisowurtzitane (CL-20) and found that there were short-range hydrogen bonds, van der Waals forces, and remote van der Waals forces accounting for the interfacial enhancement. Deng's group inferred the electrostatic interaction between ammonium nitrate explosives and NBA, and the results showed that the N atom in the bonding agent can form a strong interaction with the H atom of ammonium nitrate explosives.[13] Therefore, theoretical simulations proved that the introduction of NBA should be an effective way to improve the interfacial interaction in energetic composites. Two types of bonding agents (NPBA-1 or NPBA-2) were designed using 1,3,5,7-tetranitro-1,3,5,7-tetrazocane (HMX) propellants, and the strength and elongation of modified formulations were obviously improved at different temperatures (−40, 20, and 70 °C).[14] Lin et al.[15] also reported that 1,3,5-triamino-2,4,6-trinitrobenzene (TATB)-based PBX with NBA modification displayed a significant enhancement in creep resistance and mechanical strength compared to untreated explosives. Subsequently, physically precoating TATB with graphene/bonding agent also emphasized improvement in the compressive and Brazilian strength of PBX.[16] At present, the application of NBA in the field by dissolvation−precipitation method through physical effects (such as van der Waals force, hydrogen bond, mechanical interlock, etc.). As the force between the phase interface is weak,

Received: November 14, 2024
Revised: January 8, 2025
Accepted: January 31, 2025
Published: February 27, 2025

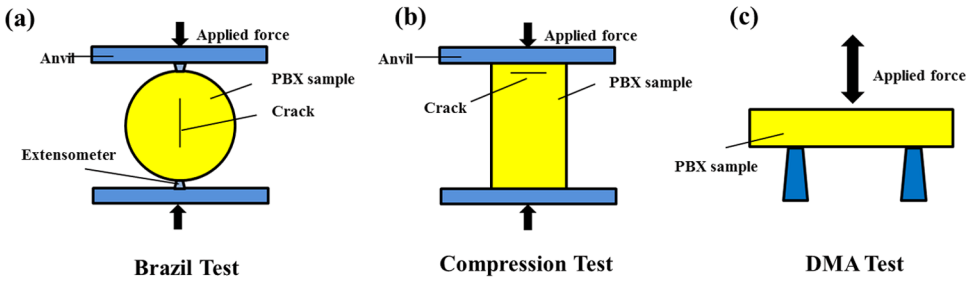

Figure 1. Mechanical measurement of (a) Brazil test, (b) compression test, and (c) DMA test.

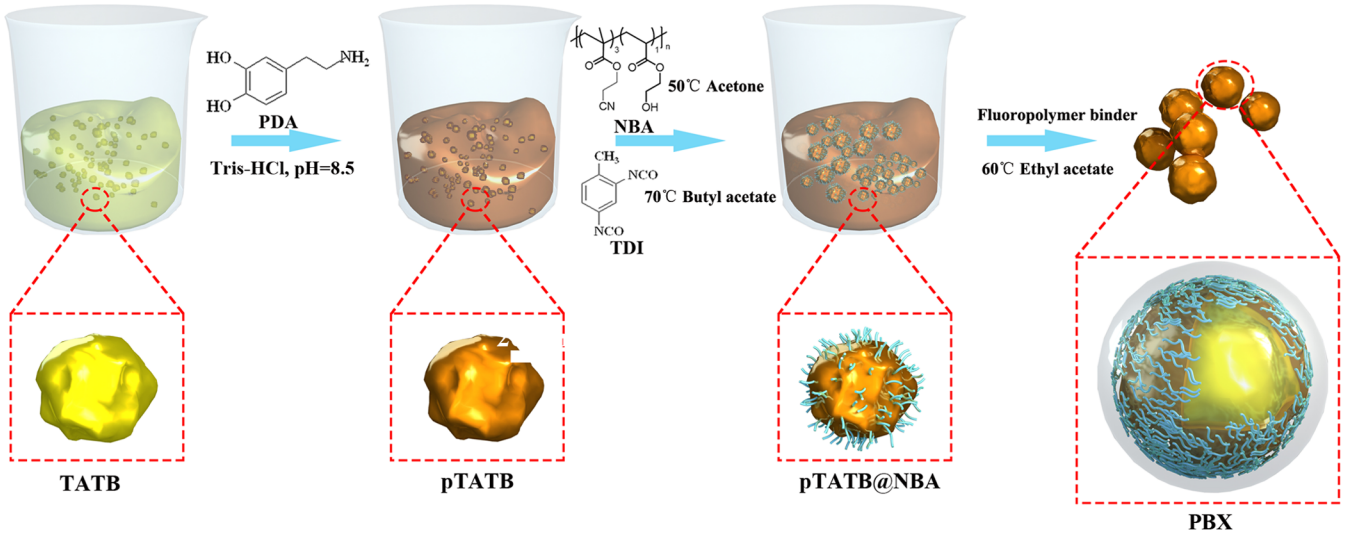

Figure 2. Schematic diagram of the pTATB@NBA preparation.

the adhesion and the thermal stability of polymer chains on the explosive surface are poor. Therefore, the ability of NBA to adjust the interface effect of PBX has certain limitations. The chemical grafting method is to covalently coat polymer on the substrate through reaction and introduce a chemical bond between the phase interface to make the intermolecular force stronger, so as to improve the bonding effect and mechanical performance.

Recently, the biomimetic coating strategy has been applied for surface engineering, designing for many high-performance composites. Dopamine (DA) has strong adhesive properties due to its abundant catechol and amino groups and forms polydopamine (PDA) shell through the self-polymerization process.[17,18] Functionalization of energetic materials based on PDA coating is widely studied, mainly due to its simple and comfortable conditions and strong bonding effect.[19−21] PDA self-polymerized by hydrogen bonding and other interactions (such as $\pi-\pi$ polymerization), effectively forming a dense coating layer on the surface of energetic crystals.[22,23] The thickness of the PDA shell can be controlled by polymerization time and catalyst, thus leading to adjustable mechanical properties, as it positively correlated with the coating thickness.[24] Furthermore, the hydroxyl and amino functional groups of PDA exposed on the surface can serve as secondary platforms for the grafting reaction.[25,26] The introduction of multilevel structure and hydrogen bonds on the explosive surface can be utilized to enhance the interaction with adhesive molecules, leading to improved mechanical properties of PBX.

In the presented work, inspired by the adhesive mechanism of mussel, the TATB crystal was first coated with the PDA shell, followed by NBA grafting. Surface and mechanical characterizations have been systematically conducted on a typical TATB-based PBX. As a result, the interfacial work was greatly improved by the synergetic effect of hydrogen bonding and physical anchor, leading to remarkably enhanced mechanical properties. The surface modification of TATB demonstrated in this paper may highlight an effective method for composite construction and mechanical enhancement.

2. EXPERIMENTAL SECTION

2.1. Reagents and Instruments. *2.1.1. Reagents.* TATB, with an average particle size of nearly 15 μm, was self-made by the Institute of Chemical Materials, Chinese Academy of Engineering Physics. The dopamine hydrochloride (DA, 98%) and (hydroxymethyl) aminomethane (Tris, 99%) were provided by Sigma Shanghai Trading Co., Ltd. The molecule involved in the grafting reaction is 2,4-toluene-diisocyanate (TDI, 99%) with a pair of −NCO groups, and it was purchased from Shanghai Aladdin Biochemical Technology Co., Ltd. The reaction catalyst is dibutyltin dilaurate (DBTDL, 95%), which was purchased from Shanghai Macklin Biochemical Technology Co., Ltd. NBA is a neutral polymer of polypropylene ester synthesized by the Shanghai Institute of Organic Chemistry. A copolymer of chlorotrifluoroethylene and vinylidene fluoride (fluoropolymer) used as a polymeric binder in the granulation process was bought from Zhonghao Chenguang Chemical Industry Co., Ltd., China. The reagents including butyl acetate, ethyl acetate, and acetone were all analytical grade (99%) and provided by Chron Chemicals Co., Ltd.

https://doi.org/10.1021/acsomega.4c10364
ACS Omega 2025, 10, 9441−9452

2.1.2. Instruments. The roughness and morphology of the TATB powder before and after modification was characterized by scanning electron microscopy (SEM) under a SE2 mode with 3 kV electron voltage. The roughness and morphology of TATB explosives before and after surface modification were measured by an atomic force microscope (AFM) using the RTESP-300 probe model and tapping mode, with a testing range of 5 × 5 μm^2. X-ray photoelectron spectroscopy (XPS) was conducted to present the chemical element on TATB and modified powder surface. The static mechanical behaviors, including Brazil and compressive tests, were performed with a universal testing system. The cylinders with sizes of Φ20 × 6 mm^2 and Φ20 × 20 mm^2 were settled at room temperature for the stress−strain curve. Also, the maximum strength and strain can be applied to evaluate the mechanical performance. The creep properties of the 30 mm × 10 mm × 2 mm sample were examined by the dynamic mechanical analysis (DMA) under a three-point bending mode. The modulus and creep curves were presented under different temperatures and stress. The schematic pictures of mechanical instruments are given in Figure 1. In order to gain a deeper insight into the enhancement mechanisms of NBA on interfacial interaction, molecular dynamics (MD) simulations were performed to quantitatively characterize the interfacial energy between NBA and different planes of the TATB crystal.

2.2. Experimental Process. TATB was first dispersed in the DA water solution to obtain PDA-coated TATB (TATB@PDA, abbreviated as pTATB), and the coating time for PDA was 6 h, corresponding to the specific process of ref 27. Then, the TDI reagent acted as a "bridge" to graft NBA on the pTATB surface (named pTATB@NBA) by using the polyurethane reaction between −OH and −NCO groups. In addition, the physical composite of TATB and NBA was also prepared for comparison. The molding powders of PBX were composites of modified TATB and fluorine-containing binder.

2.2.1. Preparation of pTATB@NBA. The schematic process of pTATB@NBA preparation is displayed in Figure 2. A 100 g portion of the pTATB explosive and 250 mL of butyl acetate were weighed into a three-jacket reactor. The installation was settled in a 70 °C water bath and under mechanical stirring of 400−600 rpm. TDI (0.5 g) and DBTDL (0.25 g) were added to the suspension successively under continuous stirring for about 1 h. Then, the powder was filtered and washed with butyl acetate, and a small amount of intermediate sample (named pTATB@TDI) was used for structural characterization. After that, the sample was dissolved in 250 mL of acetone and set in a 50 °C water bath synchronously. NBA was dissolved in acetone as the solution before use and the mixture (about 0.5 g of NBA) was dropped and the suspension stirred for another 1 h. Finally, the powder was filtered and washed with acetone three times and dried at 60 °C under vacuum to obtain pTATB@NBA (about 0.5 wt % NBA).

2.2.2. Preparation of TATB/NBA. Compared with pTATB@NBA, a physical mix of TATB and NBA (labeled as TATB/NBA) was prepared. About 100 g of TATB powders was added in deionized water in a 60 °C water bath, and the NBA solution was added dropwise. Under continuous mechanical stirring and vacuum treatment, the acetone might completely evaporate. In the end, the samples were filtered and heated to 60 °C for 8 h. The content of NBA in TATB/NBA was also 0.5 wt %.

2.2.3. Preparation of TATB-Based PBX. According to the formulation, explosive and fluorine-containing binders were first weighed and mixed in the ethyl acetate solvent with stirring at 60 °C. After the solvent had evaporated completely, the sample was further dried at 60 °C to obtain PBX powders. The specific abbreviations and components of several PBX are shown in Table 1.

Table 1. Components of TATB-Based PBX Composites

sample	components
PBX-0	TATB, fluorolymer
PBX-1	pTATB, fluorolymer
PBX-2	TATB/NBA, fluorolymer
PBX-3	pTATB@NBA, fluorolymer

Then, the different sizes of PBX pellets were prepared in steel molds under 380 MPa and 120 °C. The specific PBX with typical size is also given in Section 2.1.

2.3. Simulations of Interfacial Energies. For the interfacial energies of NBA/TATB and fluoropolymer/TATB, molecular dynamics combined with the Bravais−Friedel−Donnay−Harker (BFDH) method was used to establish the structure of TATB explosives, mainly including the crystal planes in different directions of TATB crystals.[28,29] Moreover, the molecular structures of NBA and the fluoropolymer were optimized to give a realistic state. The MD simulation conditions were a canonical ensemble (NVT) system at a temperature of 298 K and a 1 fs time step.

The binding energy between TATB, PDA, and NBA was calculated using the DMol3 module in Materials Studio 8.0, which was considered molecular bonding. Then, each component was fully relaxed using the DMol3 module and the Perdew−Burke−Ernzerhof (PBE) exchange-correlation functional of the generalized gradient approximation (GGA).[30] The precision was set to "fine", and other settings were kept as default. After structural optimization, the adsorption model was constructed using the adsorption locator tool in MS. Then, the adsorption system was freely optimized using the DMol3 module. Finally, a single-point energy calculation was performed, and the electron density and electrostatic potential were output, with the isosurface level set to 0.02 au. The interfacial energy (E_{inter}) is deduced by equilibrium conformation, and the function is given as follows

$$E_{inter} = E_{total} - (E_A + E_B) \quad (1)$$

Here, E_{total}, E_A, and E_B are the energies of the total energy and the separated components A and B, respectively.

3. RESULTS AND DISCUSSION

3.1. Surface Morphology and Structure of Explosives. The surface morphology of TATB explosives before and after modification was examined by SEM, and the pictures are shown in Figure 3. From Figure 3a, the TATB crystal exhibited a pagoda-like shape and layered stacking characteristics, with an average particle size of approximately 10−20 μm. The surface of TATB was relatively smooth and flat, only with some small cracks in magnification. After coating with PDA, TATB crystals aggregated and the roughness of the TATB surface changed in Figure 3c,d. The surface became very rough after NBA grafting onto pTATB, and more cracks appeared, as displayed in Figure 3f. The hierarchical structure of PDA deposition and NBA brush may account for the increased roughness.

The surface morphology and roughness of the TATB samples were further characterized by AFM measurements (Figure 4). As given in Figure 4a, the neat TATB displayed a relatively flat surface without modification, which was consistent with the

https://doi.org/10.1021/acsomega.4c10364
ACS Omega 2025, 10, 9441−9452

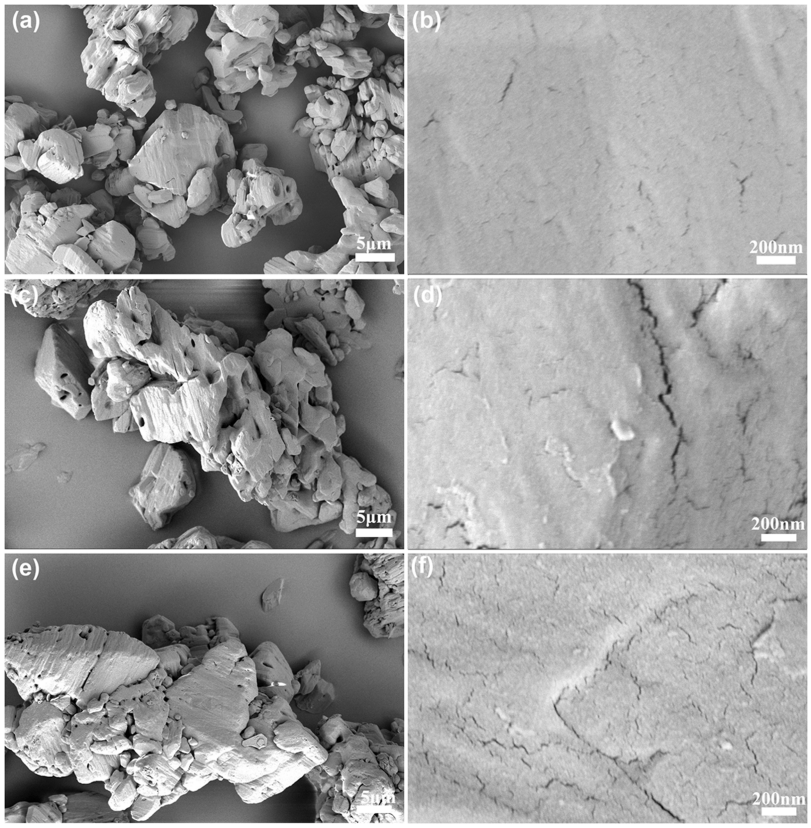

Figure 3. TATB powder before and after modification: (a, b) TATB, (c, d) pTATB, and (e, f) pTATB@NBA.

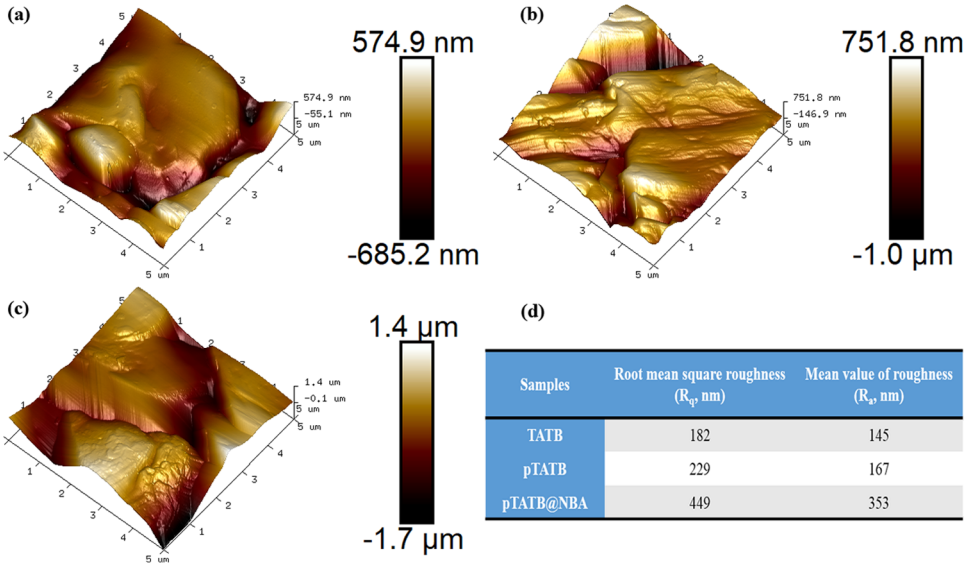

Samples	Root mean square roughness (R_q, nm)	Mean value of roughness (R_a, nm)
TATB	182	145
pTATB	229	167
pTATB@NBA	449	353

Figure 4. Topographical AFM images of (a) TATB, (b) pTATB, and (c) pTATB@NBA and (d) the roughness of the TATB samples.

result of SEM. After coating with PDA, the surface of TATB was densely covered with PDA aggregation, leading to a rough surface morphology (Figure 4b). The fluctuation appeared when being grafted with NBA, more chains gathered on the surface to form a "polymeric brush," which resulted in the severe roughness of the TATB surface.[31] In addition, the quantitative roughness including average roughness (R_a) and root-mean-square (R_q) from AFM pictures is measured in Figure 4d. Compared to 135 nm for the pristine TATB surface, the R_a significantly increased to 167 nm for pTATB samples and 353 nm for the pTATB@NBA surface. The phenomenon was mainly attributed to the surface deposition of PDA conjugation and the brush of the NBA network, which helped in achieving enhanced mechanical properties.

The elemental states on the TATB surface were determined by XPS spectroscopy, and the typical high-resolution spectra of the C 1s, N 1s, and O 1s regions are presented in Figure 5. For raw TATB, there were C−NO_2, C−NH_2, and C−C peaks in the C 1s pattern with corresponding binding energies of 287.2, 286.0, and 284.6 eV. The N 1s spectra of Ph-NO_2 and Ph-NH_2 at

https://doi.org/10.1021/acsomega.4c10364
ACS Omega 2025, 10, 9441−9452

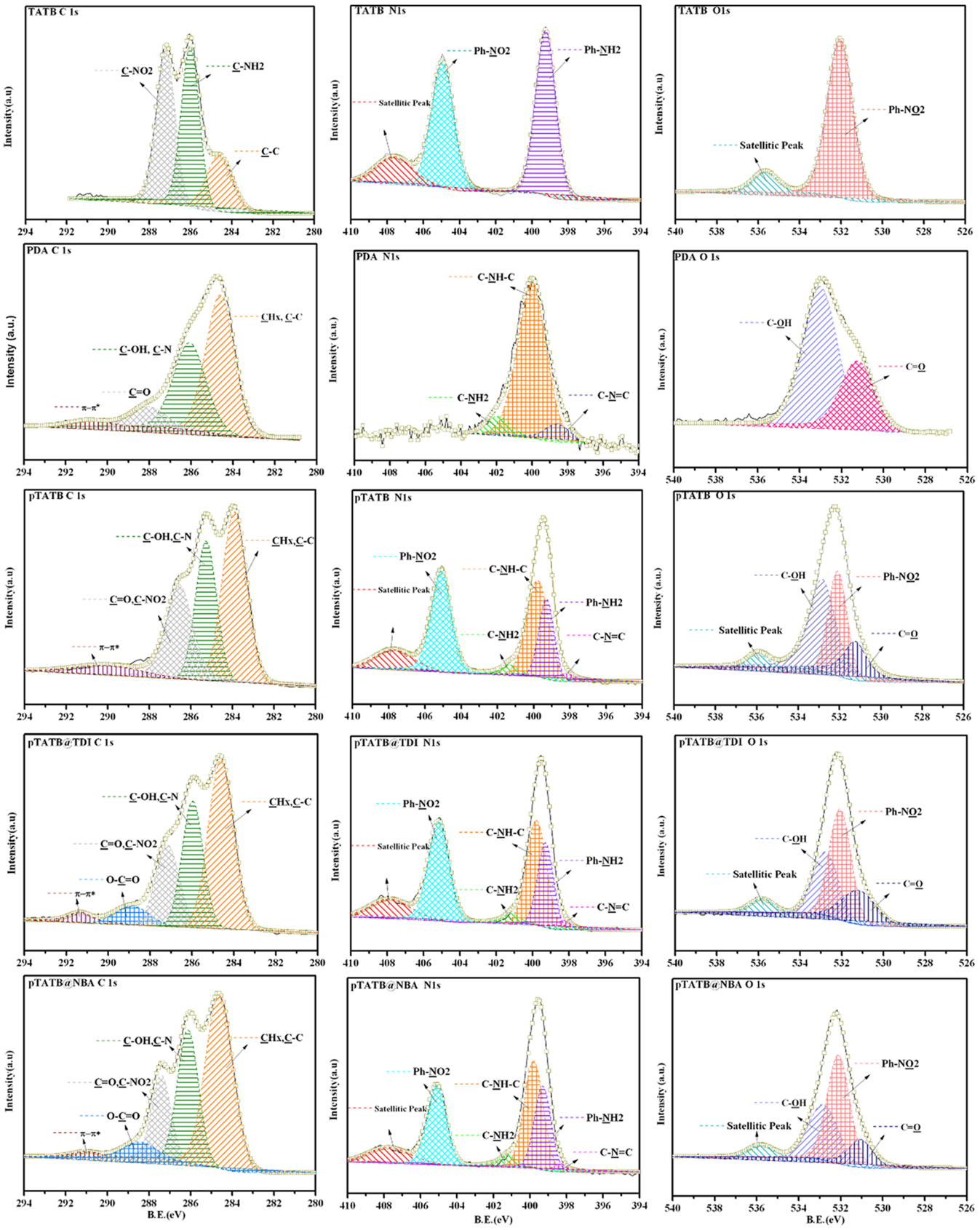

Figure 5. XPS spectra of the TATB powder before and after modification.

about 404.9 and 399.3 eV, respectively, represented the vibrations of the benzene ring. Meanwhile, there was a satellite peak of N 1s at 407.7 eV. The peaks at 535.7 and 532.1 eV in the O 1s spectrum were satellite peak and Ph-NO_2 in TATB, respectively. The PDA powder was obtained by the oxidation polymerization of dopamine in water, and its C 1s mainly

https://doi.org/10.1021/acsomega.4c10364
ACS Omega 2025, 10, 9441−9452

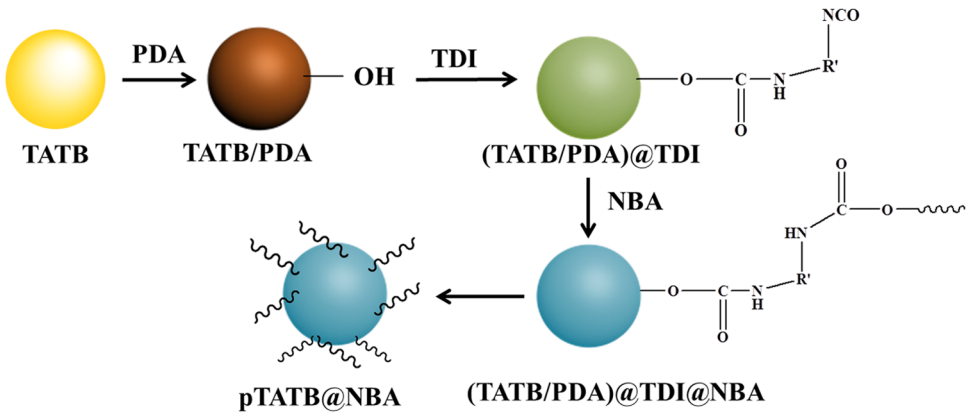

Figure 6. Schematic diagram of the Grafting Reaction for pTATB@NBA.

included the C−C peak at 284.6 eV, C−N peak at 286.1 eV, C═O at 288.1 eV, and $\pi-\pi^*$ shakeup at 290.7 eV. The N 1s peak typically contained three peaks, which were named C═N−C at 398.6 eV, C−NH−C at 400.0 eV, and C−NH at 401.9 eV. The main peaks of the O 1s spectrum were C−O and C═O, with corresponding peaks of 531.2 and 533.0 eV.

After coating with PDA, the peak station of pTATB can be regarded as the superposition of TATB and PDA only with some differences in the peak intensify. pTATB@TDI was an intermediate product during the grafting process, mainly to prove the effective introduction of TDI. The basic peaks of pTATB@TDI in the N 1s and the O 1s spectra were consistent with those of pTATB, while a new bond of the ═C═O existed in the C 1s pattern. In addition, the O−C═O peak also appeared in the pTATB@NBA sample, indicating the successful grafting reaction between −OH and −NCO in TDI to form the −NHCOO bond. The specific mechanism of the grafting reaction is schematically described in Figure 6. It is worth noting that the intensity of the C−OH peak in the O 1s graph decreased, which was due to the consumption of −OH bonds in the grafting reaction.

3.2. Mechanical Properties of PBX. The modulus and loss factor in dynamic mechanics under oscillating force can be characterized by DMA, which is an effective method of analyzing the interface structure−polymer movement−creep properties based on the viscoelasticity of composite materials. The creep curves of TATB-based PBXs were performed at different temperatures (30, 45, 60, 75 °C) under 3 MPa and different stresses (4, 7, 9 MPa), as shown in Figure 7. The typical strain curve of PBX can be divided into two stages, instantaneous elastic strain and stable creep strain. The strain of the raw PBX gradually enhanced with the increase in temperature and the shortened stable strain stage (Figure 7a). It is worth emphasizing that PBX-0 did not break at 75 °C and 3 MPa, and the stable strain was close to 8×10^{-4}. After PDA (Figure 7c) or NBA modification (Figure 7e), the creep strain of PBX significantly decreased under all temperatures, with the maximum strain below 5×10^{-4}. Generally, PBX-2 exhibited low strain when the temperature was under 60 °C, indicating the bonding effect of NBA on interfacial reinforcement. Especially for the PBX-3 sample, the strain did not exceed 3.5×10^{-4} at 75 °C, as shown in Figure 7g. The synergetic hydrogen bonding among PDA, NBA, and the fluoropolymer may be responsible for the improved creep resistance. Meanwhile, the polymeric network produced by grafted chains may hinder the slip of adhesive molecules, leading to an extremely low creep strain overall.

The creep deformation of PBXs depending on the pressure was more significant than that on the temperature, as provided in Figure 7b. PBX-0 experienced failure before entering a stable strain at 9 MPa, while it was not broken under other pressures. For the pTATB-based sample, the maximum strain of PBX-1 was about 11×10^{-4} under 9 MPa, and the strains under 7 and 4 MPa were obviously lower than those of PBX-0 (Figure 7d). It is worth noting that the TATB/NBA sample has more creep resistance compared with PBX-1 under 9 MPa, with maximum strain below 6×10^{-4}. For pTATB@NBA-based PBX, the creep strain was obviously suppressed especially at 4 MPa, which was the lowest among all stresses, and may result from enhanced interfacial work by PDA and NBA.

In the process of long-term storage and use, PBX will deform under the influence of an external load and temperature. The creep behaviors can be tested at higher temperatures for a short period of time as well as at lower temperatures for a long period of time. The time−temperature equivalence principle suggested that the mechanical properties of viscoelastic materials at different time scales can be achieved by changing the temperature.[32] Short-term experimental data was used to estimate the relatively long-term creep performance, providing an accelerated characterization method for studying PBX materials. Based on the Williams−Landel−Fery (WLF) and Boltzmann superposition principle equations,[33,34] PBX at a reference temperature of 30 °C and a stress of 4 MPa was adopted as the initial principal curve for time−temperature equivalence. The remaining curves were moved horizontally in the order of temperature from low to high and finally, the principal curves were obtained, as illustrated in Figure 8a. The strain was generally increased with increasing time, but PBX-0 showed a rapid increase in amplitude for the whole time. For the convenience of comparison, a period of approximately 1 month was selected, and the corresponding strains for all samples were 5.01×10^{-4} (PBX-0), 4.02×10^{-4} (PBX-1), 3.73×10^{-4} (PBX-2), and 3.28×10^{-4} (PBX-3). It can be seen that after surface modification, the extrapolated strain of PBX was lower than that of PBX-0 at 1 month. The introduction of PDA and NBA significantly inhibited the strain of the explosive, reducing the long-term strain by about 34.5%.

The storage modulus (E) was an index for the stiffness of PBX, and the results of different PBXs within a temperature range of 20−120 °C are illustrated in Figure 8b. Overall, E gradually decreased with increasing temperature for all PBXs. The modulus of PBX-1 and PBX-2 at 20 °C was close to 7000 MPa, which was obviously higher than that of PBX-0 (about

https://doi.org/10.1021/acsomega.4c10364
ACS Omega 2025, 10, 9441−9452

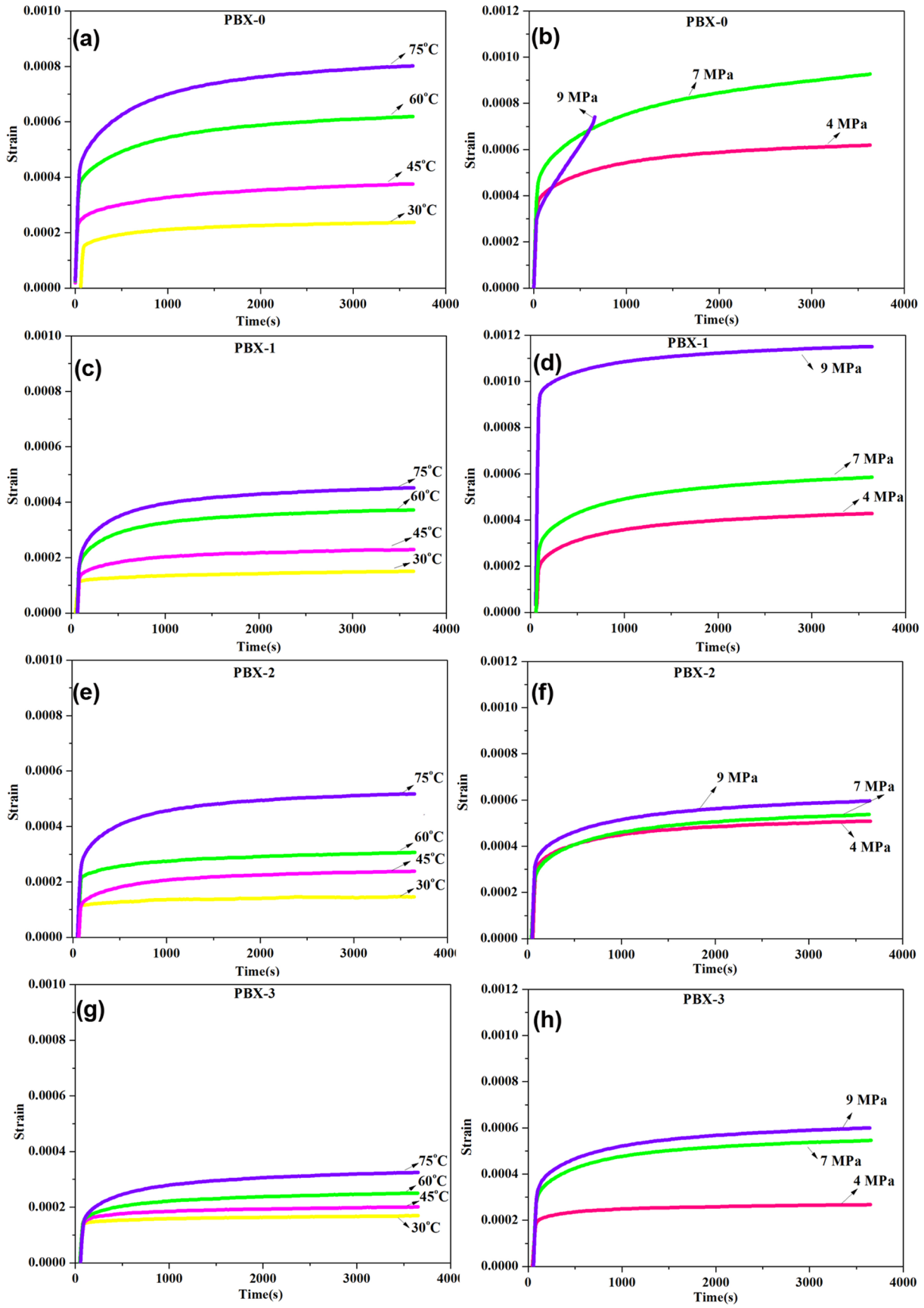

Figure 7. Creep strain curve of TATB-based PBXs at different temperatures and stresses: (a, b) PBX-0, (c, d) PBX-1, (e, f) PBX-2, and (g, h) PBX-3.

https://doi.org/10.1021/acsomega.4c10364
ACS Omega 2025, 10, 9441−9452

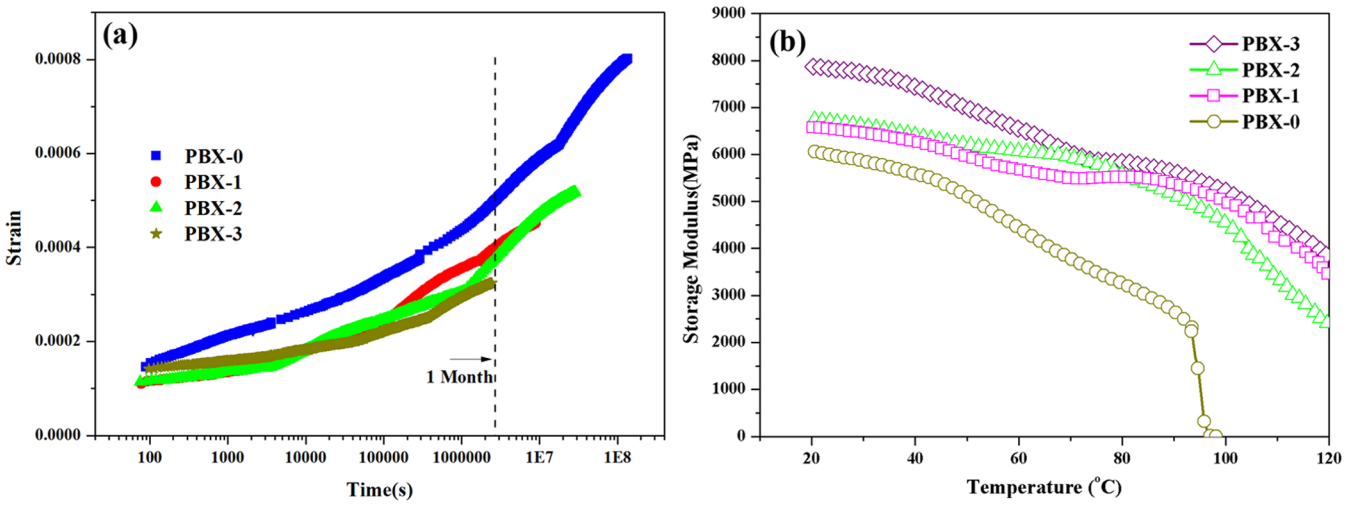

Figure 8. (a) Long-term creep curves of different TATB-based PBXs at 30 °C, 3 MPa, and (b) storage modulus at 20−120 °C range.

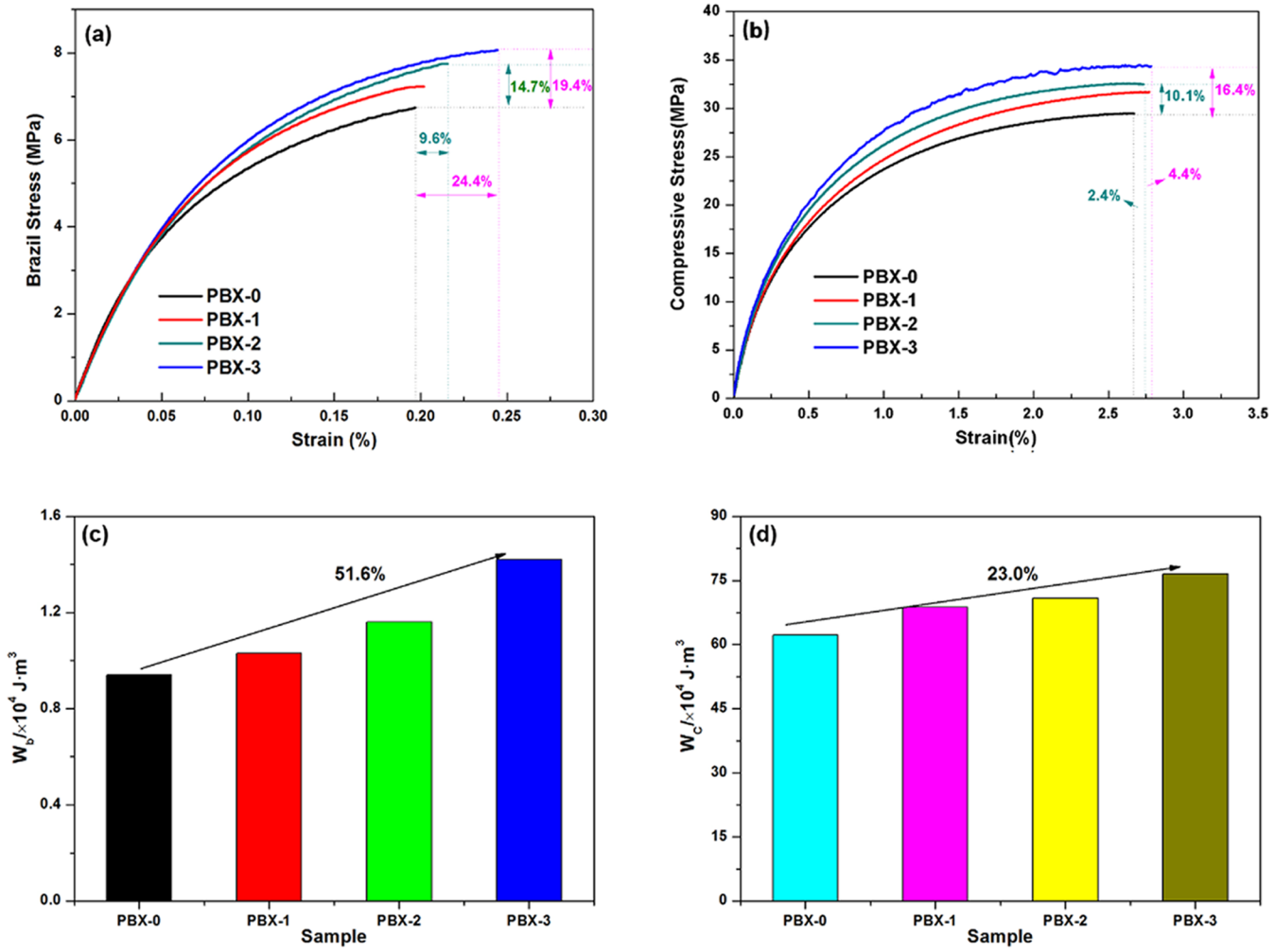

Figure 9. (a) Brazil properties, (b) compressive properties, (c) Brazil fracture energy, and (d) compressive fracture energy of different TATB-based PBXs.

6000 MPa). Also, PBX-1, with a value of about 3000 MPa, displayed a slightly higher *E* than that of PBX-2. With a further combination of PDA coating and NBA grafting, the *E* of PBX-3 was nearly 7500 MPa around room temperature, pronouncing a good reinforcement in the interfacial work of PBX. When the temperature increased, the movement of the molecular chain intensified, causing slip and deformation of the binder. PBX-0 was broken when the temperature increased above 95 °C, while the modified samples displayed an apparent improvement in the modulus at high temperatures, especially for PBX-3 with the *E*

https://doi.org/10.1021/acsomega.4c10364
ACS Omega 2025, 10, 9441−9452

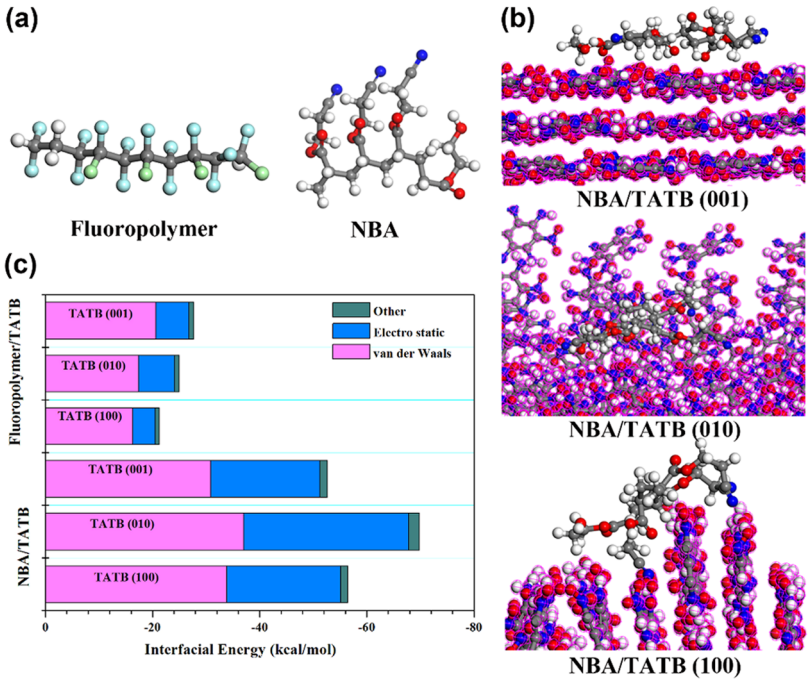

Figure 10. (a) Model of fluoropolymer and NBA molecules, (b) model of the interface between NBA and TATB crystal planes, and (c) interface interaction energy of fluoropolymer/TATB and NBA/TATB at different crystal planes.

value of nearly 3800 MPa at 120 °C. The physical anchoring points and hydrogen bonding produced by the polymer brush of NBA may limit the movement of binders and enhance the storage modulus of PBXs.

As the highly loaded composites of PBX, the brittle materials were used for the measurement of static mechanics, and the response of mechanical performance of different TATB-based PBXs is given in Figure 9. Compared with PBX-0, pTATB-based PBX (PBX-1) showed much higher strength and elongation due to the rough surface formed by PDA and the reinforced interaction between functional bonds and binders.[35,36] The bonding effect of NBA has a better interfacial interaction compared with PDA, which showed 14.7 and 10.1% enhancement in strength, respectively. Moreover, TATB was modified by PDA coating, followed by NBA grafting, and the Brazil (tensile) and compressive strength of PBX-3 increased visibly, reaching the maximum strength with the enhancement of 19.4 and 16.4%, respectively. Also, in the Brazillian (tensile) and compressive elongation tests, PBX-3 presented 24.4 and 4.4% improvement, respectively, which may be attributed to the hierarchical structure of PDA and NBA modification.[37]

To quantitatively analyze the mechanical properties of PBXs before and after modification with PDA and NBA, the toughness of the explosives was characterized by Brazilian (tensile) fracture energy (W_b) and compressive fracture energy (W_c), mainly represented by the integral area of stress−strain curves. The integration formula used can be expressed as follows

$$W_b = \int_0^{\varepsilon_b} \sigma_b \, d\varepsilon \tag{2}$$

$$W_c = \int_0^{\varepsilon_c} \sigma_c \, d\varepsilon \tag{3}$$

Here, ε_b and ε_c were the maximum strain values when PBX once broke. According to eqs 2 and 3, the results of W_t and W_c are shown in Figure 9c,d, respectively. From the definition, fracture work referred to the energy absorbed per unit volume when the sample fractured, from which the mechanical performance was relatively consult. The fracture energy of PBX was found to be consistent with the mentioned mechanical properties. Consistently, the fracture toughness of PBX was increased after surface modification of TATB. For example, the W_t of PBX-0 was approximately 0.94×10^{-4} J/m, while the value increased to 1.03×10^{-4} J/m after coating with PDA. For the NBA-coated sample, the W_t was 0.94×10^{-4} J/m, which was slightly enhanced compared with that of PBX-1. Further grafting with NBA, the value of fracture energy was 1.42×10^{-4} J/m, which was an increase of 51.6% compared to that of PBX-0. Meanwhile, the compressive fracture energy increased from 62.21×10^{-4} J/m for PBX-0 to 76.5 J/m for PBX-3, equivalent to about 23.0% improvement.

3.3. Simulated Calculation of Interfacial Energy. Surface modification of TATB can improve the interfacial interaction between explosives and binders, thereby improving the mechanical properties of PBX. Early report has investigated the surface interaction between PDA and different TATB crystal surfaces, and the results showed that the PDA shell contributes much to the interfacial effect due to its strong adhesion.[38] It is also worth noting that the interfacial interaction of fluoropolymer/PDA was much lower than that of PDA/TATB, thus the interfacial energies of fluoropolymer/PDA and fluoropolymer/NBA are not discussed in this work.[39] In order to further evaluate the interfacial force and enhanced mechanism in NBA-modified explosives, the interaction energies of NBA/TATB and fluoropolymer/TATB were first simulated using the MD method. Then, the equilibrium conformation of TATB/NBA composites was obtained, as shown in Figure 10b. Also, the van der Waals and electrostatic potentials were calculated, as shown in Figure 10c. The interface energies of fluoropolymer/TATB and NBA/TATB were obtained, which mainly include van der Waals forces, electrostatic potentials, and other interaction forces. Overall, the interaction energy between the three crystal

https://doi.org/10.1021/acsomega.4c10364
ACS Omega 2025, 10, 9441−9452

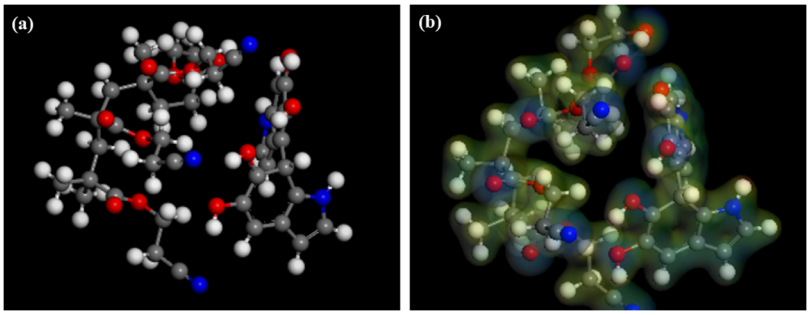

Figure 11. (a) Adsorption model and (b) model of electron density for PDA/NBA.

planes of TATB and NBA was significantly higher than that of the fluoropolymer. It should also be emphasized that the interaction between NBA and TATB exhibited anisotropy with the highest interfacial energy in the (010) crystal plane. The presence of a large number of amino and hydroxyl functional groups in NBA led to the formation of hydrogen bonds with the surface of the explosive and binders, exhibiting an overall improvement in interfacial energy.

For PDA and NBA, the binding energy of single molecules was calculated by using the DMol3 module, and the adsorption model with the electrostatic potential (ESP) mapped onto the isosurface of the electron density is provided in Figure 11. It was reported that the interfacial energy of PDA/TATB was about −20.92 kal/mol, which emphasized the improved bonding effect of PDA.[40] The value was −15.6 kal/mol for the PDA/NBA interface when $N = 1$ of the NBA polymer was chosen. From the results, NBA had good adhesion with PDA and TATB, which mainly accounted for the increased interaction of pTATB@NBA-based PBX, resulting in significant enhancement in mechanical properties.

4. CONCLUSIONS

Inspired by the achievements of nacre, the hierarchical structure including a PDA coating combined with chemical grafting was designed and prepared in response to the problem of weak interfacial interaction and low mechanical properties of PBX. The effect of surface functionalization on the surface properties and mechanical properties of TATB-based PBX was characterized through SEM, XPS, DMA, and mechanical properties. The result showed that after surface modification, the roughness of the TATB surface intensified due to the aggregation of PDA and the polymer brush. The new bond of −NHCOO formed after NBA grafting in the XPS spectrum indicated the successful covalent reaction of TDI and NBA. With the introduction of PDA and NBA, the creep strain of PBX-3 was lowered to 3.5×10^{-4} at 3 MPa and 75 °C, and it maintained good rigidity under higher stresses. Moreover, the storage modulus of PBX-3 reached 7500 MPa at 20 °C and about 3800 MPa at 120 °C. The method of PDA coating followed by NBA grafting increased the tensile strength and strain of PBX-3 by 19.4 and 24.4%, respectively. The computational results displayed that the enhanced mechanism combined with van der Waals forces, $\pi-\pi$ interaction, hydrogen bonds, and surface roughness accounted for the improvement of mechanical properties, finally leading to a 51.6% increase in the fracture energy of PBX-3. The results revealed in this work can be commonly highlighted with regard to surface modification and performance enhancement of other functional composites.

AUTHOR INFORMATION

Corresponding Authors

Chengcheng Zeng − *Institute of Chemical Materials, China Academy of Engineering Physics, Mianyang 621900, China;* orcid.org/0000-0002-3283-0100; Email: zengcc1314@caep.cn

Fude Nie − *Institute of Chemical Materials, China Academy of Engineering Physics, Mianyang 621900, China;* Email: niefude@caep.cn

Authors

Gang Li − *Institute of Chemical Materials, China Academy of Engineering Physics, Mianyang 621900, China*

Congmei Lin − *Institute of Chemical Materials, China Academy of Engineering Physics, Mianyang 621900, China;* orcid.org/0000-0001-8734-0769

Guansong He − *Institute of Chemical Materials, China Academy of Engineering Physics, Mianyang 621900, China;* orcid.org/0000-0002-0575-6486

Lixiao Hao − *Institute of Chemical Materials, China Academy of Engineering Physics, Mianyang 621900, China*

Feiyan Gong − *Institute of Chemical Materials, China Academy of Engineering Physics, Mianyang 621900, China;* orcid.org/0000-0001-8604-9515

Shengjun Zheng − *Institute of Chemical Materials, China Academy of Engineering Physics, Mianyang 621900, China*

Complete contact information is available at: https://pubs.acs.org/10.1021/acsomega.4c10364

Notes

The authors declare no competing financial interest.

ACKNOWLEDGMENTS

The authors greatly appreciate the financial support from the NSAF Joint Found (Grant Number U2130207) and the National Natural Science Foundation of China (22275173), and the Presidential Foundation of China Academy of Engineering Physics (YZJJZQ2023008).

REFERENCES

(1) Wuillaume, A.; Beaucamp, A.; Quillot, F. D.; Erades, C. Formulation and characterizations of nanoenergetic compositions with improved safety. *Propellants, Explos. Pyrotech.* **2014**, *39* (3), 390−396.

(2) Yan, Q.-L.; Cohen, A.; Petrutik, N.; Shlomovich, A.; Burstein, L.; Pangcand, S.; Gozin, M. Highly insensitive and thermostable energetic coordination nanomaterials based on functionalized graphene oxides. *J. Mater. Chem. A* **2016**, *4* (25), 9941−9948.

(3) Huang, X.; Jiang, P. Core-Shell structured high-k polymer nanocomposites for energy storage and dielectric applications. *Adv. Mater.* **2015**, *27* (3), 546−554.
(4) Yeager, J. D.; Dubey, M.; Wolverton, M. J.; Jablin, M. S.; Majewski, J.; Bahr, D. F.; Hooks, D. E. Examining chemical structure at the interface between a polymer binder and a pharmaceutical crystal with neutron reflectometry. *Polymer* **2011**, *52* (17), 3762−3768.
(5) Drodge, D. R.; Williamson, D. M.; Palmer, S. J. P.; Proud, W. G.; Govier, R. K. The mechanical response of a PBX and binder: combining results across the strain-rate and frequency domains. *J. Phys. D: Appl. Phys.* **2010**, *43* (33), 335403.
(6) Zhou, Z.; Chen, P.; Duan, Z.; Huang, F. Study on Fracture behavior of a polymer-bonded explosive simulant subjected to uniaxial compression using digital image correlation method. *Strain* **2012**, *48* (4), 326−332.
(7) Zheng, X.; Wang, J.; Yu, S. J.; Li, Y. Micro-damage in PBX and its influence on sensitivity. *Mater. Prot.* **2014**, *47* (S1), 166−171.
(8) Lin, C.-m.; Bai, L.; Yang, Z.; Gong, F.; Wen, Y. Research progress in thermal expansion characteristics of TATB based polymer bonded explosives. *Energ. Mater. Front.* **2023**, *4*, 178−193.
(9) Qi, X. F.; Xie, W. X.; Yan, Q. L.; Liu, Q.; Liu, C. Interfacial interaction between NPBA and HMX. *Acta Armament.* **2017**, *38* (010), 1942−1949.
(10) Sun, L. J.; Chang, S. J.; Yang, X. Q.; Liu, X. Research progress of neutral polymeric bonding agent. *Chem. Propellants Polym. Mater.* **2016**, *14* (1), 44−49.
(11) Yu, Z. F.; Yao, W. S.; Tan, H. M.; Cui, G. L. Mesoscopic molecular simulation of phase separation of NPBA in energetic plasticizer/prepolymer. *Chin. J. Energ. Mater.* **2016**, *24* (5), 469−478.
(12) Qin, L. X. The Interaction between the block type neutral polymer bonding agent and the CL-20 surface. *Mod. Ind. Econ. Inform.* **2021**, *11*, 15−18.
(13) Chen, J.; Meng, D.; Zhang, P.; Deng, J. Interactions between a neutral polymeric bonding agent and nitramine explosives and their influencing factors. *Energ. Mater. Front.* **2024**, *5*, 248.
(14) Wu, Z.; Zhang, J.; Xu, S.; Li, H.; Zhou, H.; Zheng, J.; Pang, A.; Yang, Y. Synthesis of two novel neutral polymeric bonding agents to enhance the mechanical properties of composite solid propellants. *RSC Adv.* **2022**, *12* (31), 19946−19952.
(15) Lin, C.; Liu, J.; He, G.; Chen, L.; Huang, Z.; Gong, F.; Liu, Y.; Liu, S. Non-linear viscoelastic properties of TATB-based polymer bonded explosives modified by a neutral polymeric bonding agent. *RSC Adv.* **2015**, *5* (5), 35811−35820.
(16) Lin, C.; He, G.; Liu, J.; Pan, L.; Liu, S. Enhanced non-linear viscoelastic properties of polymer bonded explosives based on graphene and a neutral polymeric bonding agent. *Cent. Eur. J. Energ. Mater.* **2017**, *14* (4), 788−805.
(17) Sever, M. J.; Weisser, J. T.; Monahan, J.; Srinivasan, S.; Wilker, J. J. Metal-mediated cross-linking in the generation of a marine-mussel adhesive. *Angew. Chem., Int. Ed.* **2004**, *43* (4), 448−450.
(18) Liu, Y.; Ai, K.; Lu, L. Polydopamine and its derivative materials: synthesis and promising applications in energy, environmental, and biomedical fields. *Chem. Rev.* **2014**, *114* (9), 5057−5115.
(19) Herman, M. J.; Bull, M. R.; Watkins, E. B.; Hooks, D. E.; Miller, N. A.; Liu, C.; Yeager, J. D. Structural properties of aqueous grown polydopamine thin films determined by neutron reflectometry. *Polymer* **2023**, *284* (1), No. 126272.
(20) Sivasundarampillai, J.; Youssef, L.; Priemel, T.; Mikulin, S.; Eren, E. D.; Zaslansky, P.; Jehle, F.; Harrington, M. J. A strong quick-release biointerface in mussels mediated by serotonergic cilia-based adhesion. *Science* **2023**, *382*, 829−834.
(21) Xue, Z. H.; Xu, R. X.; Wang, Z. K. P.; Yu, M. H.; Zhao, X.; Yan, Q. L. Interfacial self-assembling of nano-TATB@PDA embedded football-like CL-20 co-particles with reduced sensitivity. *Chem. Eng. J.*, **2024**, *488*, No. 151010.
(22) He, G.; Yang, Z.; Pan, L.; Zhang, J.; Liu, S.; Yan, Q. Bioinspired interfacial reinforcement of polymerbased energetic composites with a high loading of solid explosive crystals. *J. Mater. Chem. A* **2017**, *5*, 13499.
(23) Lin, C.; Gong, F.; Qian, W.; Huang, X.; Tu, X.; Sun, G.; Bai, L.; Wen, Y.; Yang, Z.; Li, J.; Guo, S. Tunable interfacial interaction intensity: Construction of a bio-inspired interface between polydopamine and energetic crystals. *Compos. Sci. Technol.* **2021**, *211*, No. 108816.
(24) Zhu, Q.; Xiao, C.; Li, S.; Luo, G. Bioinspired fabrication of insensitive HMX particles with polydopamine coating. *Propellants, Explos. Pyrotech.* **2016**, *41* (6), 1092−1097.
(25) Zeng, C.; Yang, Z.; Liu, J.; Ding, L.; Hao, S.; Gong, F.; Yang, Z. Study on Mechanical Improvement of CL-20 Energetic Co-Crystals Based PBX by Surface Modification. *Propellants, Explos. Pyrotech.* **2023**, *48*, No. e202200154.
(26) He, G.; Li, X.; Bai, L.; Meng, L.; Dai, Y.; Sun, Y.; Zeng, C.; Yang, Z.; Yang, G. Multilevel core-shell strategies for improving mechanical properties of energetic polymeric composites by the "grafting-from" route. *Composites, Part B* **2020**, *191*, No. 107967.
(27) Yang, X.; Gong, F.; Zhang, K.; Yang, W.; Zeng, C.; Yang, Z. Enhanced Creep Resistance and Mechanical Properties for CL-20 and FOX-7 based PBXs by Crystal Surface Modification. *Propellants, Explos. Pyrotech.* **2021**, *46*, 572−578.
(28) Deng, S.-c.; Luo, Y.; Qu, Y.; Yang, X.; Yang, Z.; Zhao, X.; Liu, Y.; Nie, F. Improving the mechanical performances of polymer bonded explosives using monomer tuned polythioureas. *Energ. Mater. Front.* **2023**, *4*, 85−92.
(29) Sun, S.; Guo, X.; Pan, Q.; Zhang, H.; Zhao, W.; Wu, C.; Li, S. Inhibition of dissolution-induced crystal transformation of e-Hexanitrohexaazaisowurtzitane in plasticizers by polydopamine coating. *Propellants, Explos., Pyrotech.* **2023**, *48*, No. e202200255.
(30) Qu, Z.; Muhammad, Y.; He, W.; He, W.; Li, J.; Gao, Z.; Fu, J.; Shah, S. J.; Sun, H.; Wang, J.; Huang, Z.; et al. Designing C-Fe-O bonded MIL- 88B (Fe)/jasmine petal-derived-carbon composite biosensor for the simultaneous detection of dopamine and uric acid. *Chem. Eng. J.* **2021**, *404*, No. 126570.
(31) Zhang, X.; Zhang, C.; Zhang, C.; Zhao, X.; Zhao, X.; Yang, Z. J.; Yang, Z. J.; Yan, Q. L. Desensitization and stabilization of HMX crystals by intercalation of crosslinked graphene oxide. *Chem. Eng. J.* **2024**, *502*, No. 158192.
(32) Aklonis, J. J.; Macknight, W. J. *Introduction to Polymer Viscoelasticity*; Science Press: Beijing, 1986; pp 47−58.
(33) Zhao, L.; Yuan, H.; Zhu, X.; Wen, M.; Wen, Q. Applicability Analysis of Time-temperature-stress Equivalent Principle in Tensile Creep of TATB-Based PBX. *Chin. J. Energ. Mater.* **2022**, *30* (9), 971−977.
(34) Zheng, S.; Zeng, C.; Gong, F.; Xing, C.; Lv, L.; Yang, Z.; Luo, Y.; Nie, F. Improvement of mechanical properties of TATB-based polymer bonded explosive by surface confinement and interfacial strengthening. *Surf. Interfaces* **2024**, *52*, No. 104896.
(35) Gao, F.; Jing, J.; Cheng, W.; Song, H.; Li, S.; Zhang, Z.; Wang, J.; An, C. Molecular dynamics simulation of bilayer core-shell structure of CL-20 surface-modified by polydopamine coated with polymer binder. *Mater. Today Commun.* **2023**, *37*, No. 107099.
(36) Herman, M. J.; Liu, C.; Cady, C.; Watkins, E. B.; Miller, N. A.; Duquea, A. L.; Yeager, J. D. Biologically inspired reinforcement using polydopamine of polymer bound composites. *Composites, Part B* **2023**, *254* (1), No. 110563.
(37) Jia, K. H.; Wu, P. F.; Qin, W. L.; Yu, Y. W.; Jing, S.; Cheng, G. M.; Liu, Y. C. Preparation of HMX@NPBAs microparticles by coating process with improved mechanical properties, thermal stability, and safety performance. *Can. J. Chem.* **2023**, *101* (12), 922−932.
(38) Urbelis, J. H.; Swift, J. A. Solvent Effects on the Growth Morphology and Phase Purity of CL-20. *Cryst. Growth Des.* **2014**, *14*, 1642−1649.
(39) Lin, C.; Liu, S.; Qian, W.; Gong, F.; Zhao, X.; Pan, L.; Zhang, J.; Yang, Z.; Li, J.; Guo, S. Controllable tuning of energetic crystals by bioinspired polydopamine. *Energ. Mater. Front.* **2020**, *1*, 59−66.
(40) Lin, C.; Wen, Y.; Wei, L.; Wei, L.; Liu, R.; Tu, X.; Huang, S.; Zhang, C.; Qian, W.; Bai, L.; Chen, L. Construction of zirconium tungstate modified polymer bonded energetic composites with highly

https://doi.org/10.1021/acsomega.4c10364
ACS Omega 2025, 10, 9441−9452

inhibited thermal expansion via bioinspired interfacial reinforcement.
Composites, Part A **2023**, *175*, No. 107794.

https://doi.org/10.1021/acsomega.4c10364
ACS Omega 2025, 10, 9441−9452